RESEARCH ARTICLE

# Impact of nanodisc lipid composition on cell-free expression of proton-coupled folate transporter

**Hoa Quynh Do**[1], **Carla M. Bassil**[1,2], **Elizabeth I. Andersen**[1], **Michaela Jansen**[1]*

**1** Department of Cell Physiology and Molecular Biophysics and Center for Membrane Protein Research, School of Medicine, Texas Tech University Health Sciences Center, Lubbock, Texas, United States of America, **2** The Clark Scholar Program, Texas Tech University, Lubbock, TX, United States of America

* michaela.jansen@ttuhsc.edu

**Data Availability Statement:** All relevant data are within the manuscript and its Supporting Information files.

## Abstract

The Proton-Coupled Folate Transporter (PCFT) is a transmembrane transport protein that controls the absorption of dietary folates in the small intestine. PCFT also mediates uptake of chemotherapeutically used antifolates into tumor cells. PCFT has been identified within lipid rafts observed in phospholipid bilayers of plasma membranes, a micro environment that is altered in tumor cells. The present study aimed at investigating the impact of different lipids within Lipid-protein nanodiscs (LPNs), discoidal lipid structures stabilized by membrane scaffold proteins, to yield soluble PCFT expression in an *E. coli* lysate-based cell-free transcription/translation system. In the absence of detergents or lipids, we observed PCFT quantitatively as precipitate in this system. We then explored the ability of LPNs to support solubilized PCFT expression when present during in-vitro translation. LPNs consisted of either dimyristoyl phosphatidylcholine (DMPC), palmitoyl-oleoyl phosphatidylcholine (POPC), or dimyristoyl phosphatidylglycerol (DMPG). While POPC did not lead to soluble PCFT expression, both DMPG and DMPC supported PCFT translation directly into LPNs, the latter in a concentration dependent manner. The results obtained through this study provide insights into the lipid preferences of PCFT. Membrane-embedded or solubilized PCFT will enable further studies with diverse biophysical approaches to enhance the understanding of the structure and molecular mechanism of folate transport through PCFT.

## Introduction

Folate, also known as vitamin B9, is needed to synthesize purine, thymidylate, and methionine, which are essential in cell growth and division. In mammals, there is no *de novo* folate synthesis due to the absence of the folate synthase enzymes [1]. Instead, folate is obtained from dietary sources. Folate cannot permeate membranes directly due to its hydrophilic nature, and multiple membrane transport proteins, such as the folate receptor alpha (FRα) [2, 3], reduced folate carrier (RFC) [4], and proton-coupled folate transporter (PCFT) [5–7], transport this molecule into mammalian cells. PCFT is the primary transporter for dietary folate uptake in

**Abbreviations:** PCFT, Proton-coupled folate transporter; FRα, folate receptor alpha; RFC, reduced folate carrier; HRP, horseradish peroxidase; MSP, membrane scaffold proteins; DDM, N-dodecyl β-d-maltoside; POPC, 1-palmitoyl-2-oleoyl-sn-glycero-3-phosphocholine; DMPG, 1,2-dimyristoyl-sn-glycero-3-phosphocholine; DMPC, 1,2-dimyristoyl-sn-glycero-3-phosphocholine; BME, 2-mercaptoethanol.

the gut and has a high expression level in the proximal small intestine [5, 8], i.e., in the duodenum [9] and the jejunum [10]. It is also found to be expressed in epithelial cells of the choroid plexus, where it aids the FRα-mediated transport of folate into the epithelial cytosol [11, 12]. Folate is then further transported to the cerebrospinal fluid by RFC. Loss-of-function mutations in PCFT, the mediator of the intestinal absorption and delivery of folate to the central nervous system [5, 7, 13], cause hereditary folate malabsorption [5, 14–19] with clinical and biochemical features such as diarrhea, anemia, leukopenia, cognitive and motor impairment, pneumonia, and undetectable folate levels in cerebrospinal fluid [14, 20, 21]. Cerebral folate deficiency is also connected to Alzheimer's disease[22–26] and inferred to cause epilepsy, autism spectrum disorders, and other neurological disorders in young children [27, 28]. Treatment of cerebral folate deficiency with folinic acid [19, 27, 29, 30] and its S-enantiomer levofolinic acid [21] results in clinical improvement in most patients who receive the treatment before the age of six. Folinic acid is a reduced folic acid derivative, the 5-formyl tetrahydrofolic acid, with complete vitamin activity. However, for some patients with early treatment and others with a treatment delayed beyond six years of age, incomplete neurological recovery or continuous neurological deficits have been reported [21, 27]. Therefore, toward the future development of more effective therapies for neurological disorders involving PCFT mutations, it is essential to understand the molecular mechanism of folate translocation via PCFT.

PCFT functions optimally at an acidic milieu [5, 8, 31], approximating the microenvironment of the proximal intestine and also solid tumors. Recent findings reveal the upregulation of PCFT with the highest levels in the cells derived from colorectal adenocarcinoma, ovarian carcinoma, hepatoma, and small cell lung cancer cell lines [32]. Unlike RFC, PCFT exhibits high affinity for both folic acid and 5-methyltetrahydrofolate at acidic pH ($K_m \sim$ 0.5–1 μM), and it is thus likely that PCFT is the main route by which folate enters into cancer cells. These distinctions render PCFT as an ideal candidate for targeting solid tumors.

After PCFT's initial discovery in 2006, detailed studies using mutagenesis and the substituted cysteine accessibility method predicted and confirmed a PCFT structure with 12 α-helical transmembrane segments. They also revealed amino acid residues participating in the substrate pathway and transport events [5, 10, 33–40]. These studies were complemented by structure activity studies using folate analogues including clinically used and novel synthetic antifolates[9, 41–44]. The recent cryo-EM structures obtained of chicken PCFT at 3.2–3.3Å resolution confirmed many of these results and provided detailed molecular insights into apo and pemetrexed-bound PCFT structures in [45]. Both structures are in an outward-open conformation. However, PCFT structures in different functional states and a detailed molecular understanding of PCFT's interactions with folate and antifolate compounds are lacking. To completely appreciate the dynamic cycle of folate and antifolate translocation through PCFT, detailed insights into conformational transitions are needed.

To facilitate future structure-function studies of PCFT and describe a complete translocation mechanism of folate and antifolates, we develop an approach that uses a cell-free expression system to quickly express and explore the solubilization of PCFT in the presence of preformed lipid-protein nanodiscs (LPNs). We found the highest level of soluble PCFT expression in LPNs containing DMPC lipid.

## Materials and methods

### Reagents

The pEXP5-NT/TOPO vector (Thermo Fisher) and the S30 T7 High-Yield Protein Expression System (Promega) were used to express proton-coupled folate transporter (PCFT) in vitro. POPC (Avanti Polar Lipids), DDM (Anatrace), Tween 20 (Fisher Scientific), Triton X-100

(Sigma-Aldrich), and lipid-protein nanodiscs (MSP1D1-His-POPC, MSP1D1-His-DMPG, MSP1D1-His-DMPC, Cube Biotech) were used to solubilize in-situ synthesized PCFT. A rabbit polyclonal 6X-His tag antibody conjugated to horseradish peroxidase (ab1187, Abcam) was used to detect PCFT and MSP1D1.

### Preparation of plasmid DNA

The open reading frame for full-length human proton-couple folate transporter (PCFT), Uni-ProtKB accession number Q96NT5, was cloned into the pEXP5-NT/TOPO vector to obtain PCFT-pEXP5-NT. The DNA sequence of the resulting PCFT construct contains an N-terminal 6X-His tag followed by a Tobacco Etch Virus (TEV) protease recognition site. The sequence was confirmed by DNA sequencing (Genewiz). Plasmid DNA was isolated with the EndoFree Plasmid Maxi Kit (Qiagen) following the manufacturer's protocol.

### Cell-free expression of PCFT—protein synthesis reaction

The S30 T7 High-Yield Protein Expression System was used for cell-free PCFT protein expression in the presence and the absence of LPNs, lipids, and detergents. This expression system is an *Escherichia coli* extract-based cell-free protein synthesis system, which consists of T7 RNA polymerase for transcription and all necessary components for translation.

PCFT-pEXP5-NT was used as template, which contains a T7 promoter, a ribosome binding site, and the DNA sequence encoding for full-length human PCFT protein (Fig 1). The typical reaction volume was 5 μL using the template, T7 S30 Extract for circular templates, and S30 Premix Plus as recommended by the manufacturer (Fig 2). Reactions were incubated in a thermomixer at 1,200 rpm and 37˚C for 1 hour.

Pre-assembled LPNs and/or detergents were added to some reactions. PCFT was expressed in the presence of pre-assembled LPNs consisting of the membrane scaffold protein MSP1D1-His with a single phospholipid; 1-palmitoyl-2-oleoyl-sn-glycero-3-phosphocholine (POPC), 1,2-dimyristoyl-sn-glycero-3-phosphocholine (DMPG), or 1,2-dimyristoyl-sn-gly-cero-3-phosphocholine (DMPC), MSP1D1-His-POPC, MSP1D1-His-DMPG, and MSP1D1-His-DMPC, respectively. Three different LPN concentrations were used following the LPN manufacturer's manual, 20 μM, 40 μM, and 80 μM. The mixtures were incubated for 1 hour at 37˚C before the separation of soluble and insoluble PCFT.

After the expression, each sample was centrifuged at 22,000 g for 10 min at 4˚C to separate insoluble PCFT in the pellet from soluble PCFT in the supernatant. Each pellet fraction was resuspended in 50 μL of 1x Laemmli sample buffer containing 1% SDS, with or without 2.5% of 2-mercaptoethanol. Each supernatant fraction was diluted using the same sample buffer in a total volume of 50 μL.

### Immunoblot analysis

Samples from the pellet and supernatant fractions were heated at 70˚C for 10 minutes to enhance protein denaturation. Ten microliters of each sample, which corresponds to 1 μL of the initial reaction volume, were separated on Mini-PROTEAN TGX gels (BioRad) and transferred to PVDF membranes (BioRad) using the Bio-Rad trans-blot turbo system following the manufacturer's protocol. PVDF membranes were briefly immersed in methanol and then equilibrated in western transfer buffer (20% of Bio-Rad 5x transfer buffer, 20% ethanol) for 3–5 minutes. Proteins were transferred at 2.5 Amperes and up 25 Volts for 3 minutes at room temperature. Polyvinylidene fluoride (PVDF, Biorad) membranes were blocked under agitation in 5% nonfat milk in tween-containing tris-buffered saline buffer (TTBS buffer: 0.1% Tween-20, 100 mM Tris, 0.9% NaCl, pH 7.5) for one hour or overnight. Afterwards, the blot
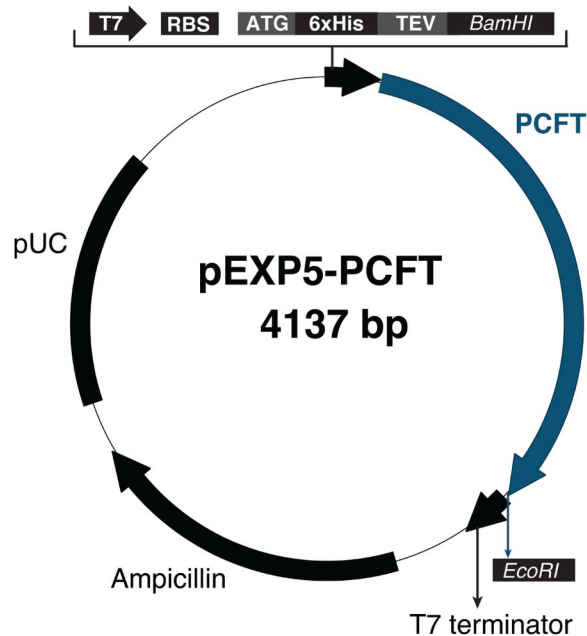
**Fig 1. PCFT expression plasmid.** The coding sequence of SLC46A1 gene, nucleotides from 99 to 1478, together with two recognition sites for BamHI and EcoRI restriction enzymes, were cloned into pEXP5-NT/TOPO vector purchased from ThermoFisher Scientific. The correct DNA sequence of the PCFT construct was confirmed by Genewiz.

https://doi.org/10.1371/journal.pone.0253184.g001

was incubated with 6X-His tag antibody conjugated with HRP in a dilution of 1:5000 for one hour under gentle agitation. Subsequently, the blot was washed five times, each for 5 minutes with 5 ml of TTBS buffer. After an additional wash with tris-buffered saline (100 mM Tris, 0.9% NaCl, pH 7.5), SuperSignal West Femto Maximum Sensitivity Substrate (Thermo Scientific) was used for imaging with a digital imaging system (ImageQuant$^{TM}$ LAS 4000, GE Healthcare).

### Data analysis

PCFT quantification was performed to determine if PCFT solubility depends on the lipid composition and concentrations of LPNs. The soluble PCFT bands on western blot images were selected, the band intensities were plotted as peaks, and the area under a peak was analyzed using ImageJ software. The resulting values were normalized to the highest value obtained from soluble PCFT expressed in LPNs. Statistical significance in PCFT solubility, depending on lipid concentrations and compositions, was determined using one-way ANOVA with Tukey's multiple-comparisons test in Prism 6 Software (GraphPad Prism, La Jolla, CA).

Data charts were generated using Microsoft Excel and Prism 6 Software (GraphPad Prism, La Jolla, CA). Figures were created using ApE plasmid editor, Adobe Illustrator 2020, and Adobe Photoshop 2020.

### Results and discussion

A detailed molecular understanding of proton-coupled folate transporter (PCFT) is desirable and essential in the structure-based design of drugs and therapies effectively targeting folate-related neurological disorders and cancer. Biochemical and biophysical techniques routinely applied to study the structure and function of proteins frequently require soluble or solubilized (membrane) proteins. For integral membrane proteins, a critical step in making protein
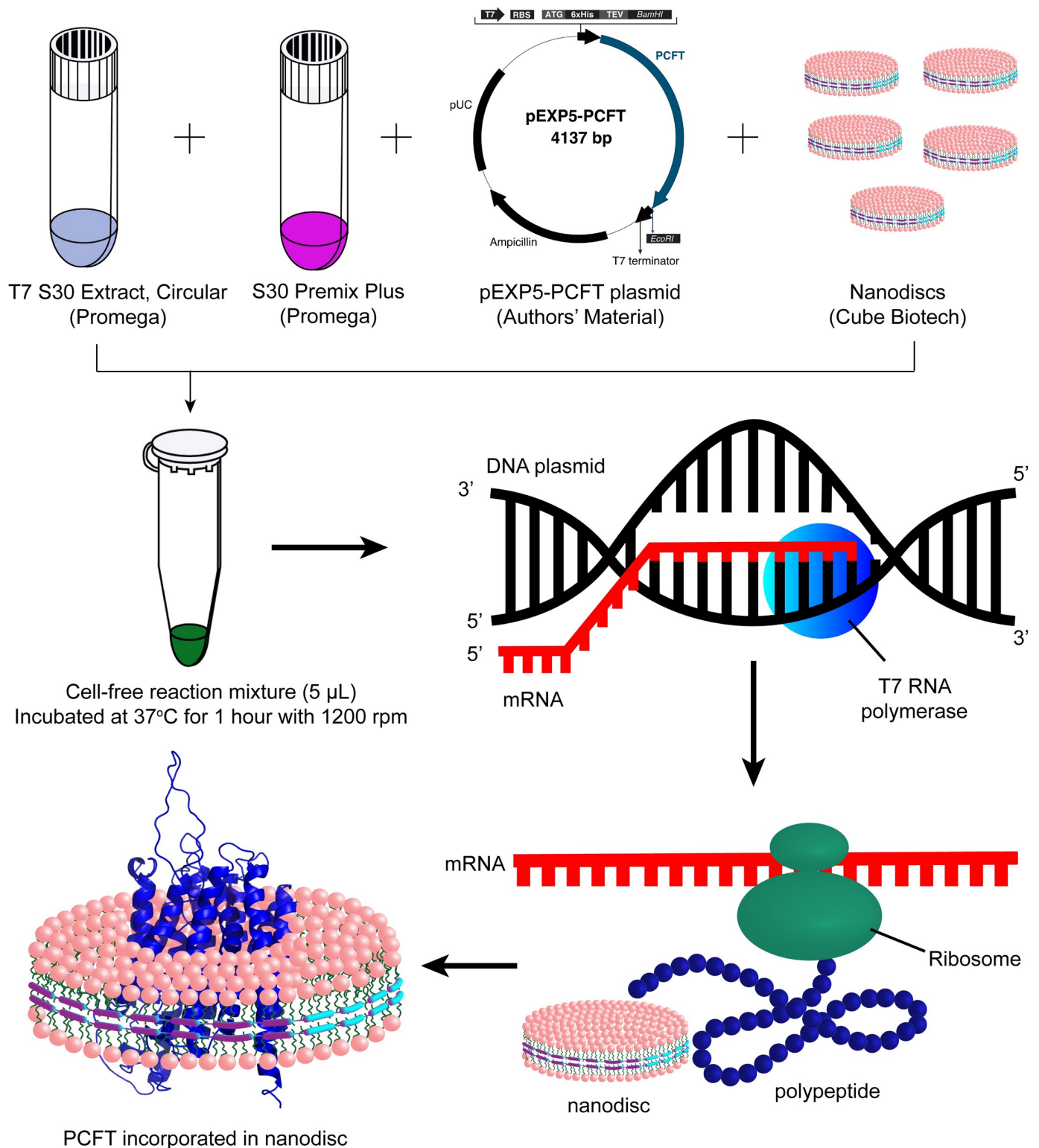
**Fig 2. Schematic for cell-free expression of PCFT in the presence of nanodiscs.** T7 S30 Extract, Circular, and S30 Premix Plus are components of the S30 T7 High-Yield Protein Expression System purchased from Promega. The pEXP5-PCFT plasmid is the PCFT construct shown in Fig 1. Empty LPNs containing POPC, DMPG, or DMPC were added to a cell-free reaction mixture. Soluble PCFT was observed when PCFT was cell-free expressed in the presence of the nanodisc.

available for biophysical approaches such as for example cryo-electron microscopy, circular dichroism, isothermal titration calorimetry, or X-ray crystallography is the solubilization of the protein from the native lipid bilayer or the integration into a stable bilayer (mimetic) or detergent micelle [46]. To produce soluble PCFT, a PCFT construct was designed as part of this study, containing full-length human PCFT cloned into the pEXP5-NT/TOPO vector (Fig 1). The cell-free transcription and translation system was then used to examine the expression and solubility of PCFT in the presence (Fig 2) or the absence of LPNs containing different lipids.

## PCFT expression is observed in cell-free expression system

Transcription/translation reactions contained PCFT-pEXP5-NT as a template. After incubation reactions were separated by centrifugation into pellet and supernatant fractions. Since PCFT is a transmembrane protein, in the absence of detergent or an otherwise solubilizing milieu, the translated protein is expected to be in the pellet, whereas soluble PCFT would be in the supernatant fraction (Fig 3). Proteins in both fractions were separated on SDS-PAGE and detected using western blotting with an antibody directed against the N-terminal 6X-His tag present in the PCFT construct.

In the absence of the plasmid PCFT-pEXP5-NT template, no band, and consequently no PCFT protein, was detected in either the pellet or supernatant fractions (Fig 3A, lanes 'Control'), whereas the presence of PCFT-pEXP5-NT template in the reaction yielded a band at approximately 37 kDa (Fig 3A, pellet fractions). The 6X-His-tagged full-length human PCFT construct in this work consists of 493 amino acids with a theoretical molecular weight of 52 kDa. When expressed in *Spodoptera frugiperda* (Sf9) insect cells [47], Chinese hamster ovary cells [34], or *Xenopus laevis* oocytes [34] monomeric PCFT migrates in two bands between 35 and 55 kDa. The electrophoretic mobility of PCFT depends on the post-translational modification of N-linked glycosylation [48]. Removing the glycosylation with PNGase F results in PCFT that mainly migrates at ~35 kDa [48]. The migration of PCFT observed here (~37 kDa) is consistent with non-glycosylated PCFT as expected in the cell-free expression system where post-translational modifications do not occur.

This data indicates that the PCFT protein was expressed in the cell-free expression system using PCFT-pEXP5-NT as a template. As would be expected in the absence of detergents or bilayers, the expressed PCFT is exclusively insoluble, and PCFT protein is only found in the pellet but not the supernatant fraction.

## Cell-free expressed and soluble PCFT is detected in the presence of LPNs

Next, the cell-free expression of PCFT was examined in the presence of LPNs of differing lipid compositions. LPNs were stabilized by the membrane scaffold protein MSP1D1 (genetically modified apolipoprotein A1 with N-terminal globular region replaced by 6X-His and Tobacco Etch Virus protease site). The ~10-nm size of MSP1D1 LPNs was used to be tailored to the diameter of a transmembrane protein with 12 α-helical transmembrane segments. Fig 3B shows PCFT translation using cell-free expression in the presence of MSP1D1 LPNs containing zwitterionic POPC with a saturated palmitoyl- and unsaturated oleoyl chain (16:0–18:1 PC; 1-palmitoyl-2-oleoyl-sn-glycero-3-phosphocholine), zwitterionic saturated DMPC (14:0 PC; 1,2-dimyristoyl-sn-glycero-3-phosphocholine) or anionic saturated DMPG (14:0 PG; 1,2-dimyristoyl-sn-glycero-3-phospho-(1'-rac-glycerol)) (Cube Biotech) with PCFT-pEXP5-NT (6X-His-PCFT) as a DNA template. In the absence of LPNs, once again only insoluble PCFT was observed. In the presence of 20 or 40 μM LPNs, PCFT was found in both insoluble form in the pellet and soluble form in the supernatant (Fig 3B). More soluble PCFT was
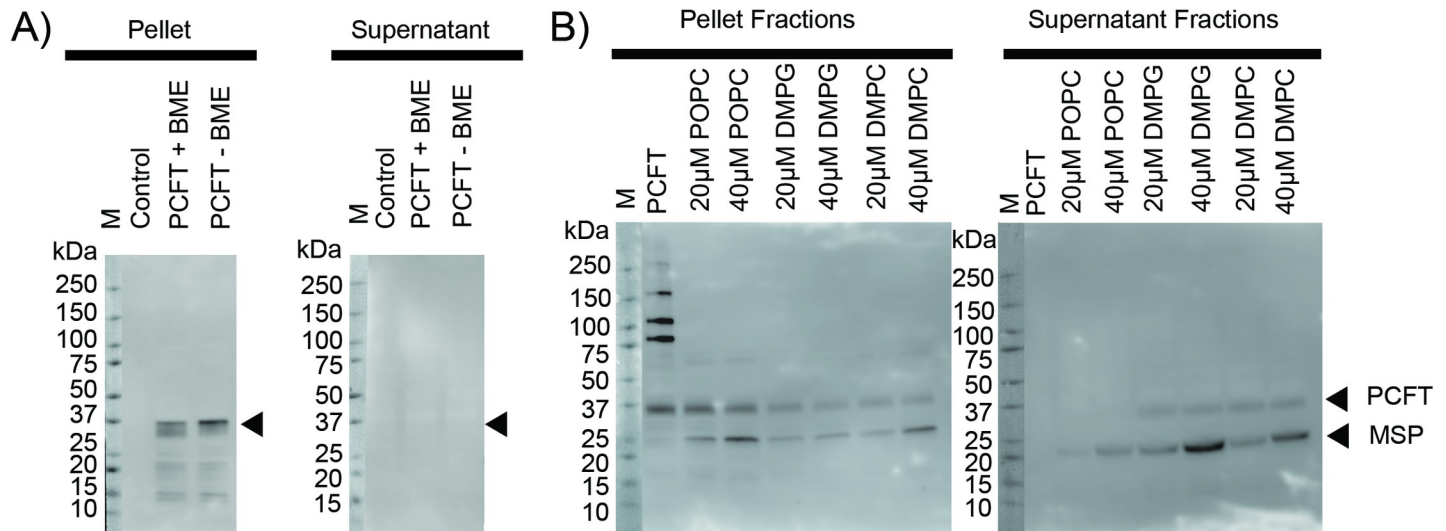
**Fig 3. Cell-free expression of Proton-Coupled Folate Transporter (PCFT).** The arrows indicate the position of monomeric PCFT (~37 kDa). A) Cell-free expression of PCFT in the absence of LPNs. The "Control" lane reactions did not contain PCFT-pEXP5-NT plasmid. $\beta$-mercaptoethanol (BME) was added to some reactions as indicated. B) Cell-free expression of PCFT in the presence of 20 μM or 40 μM LPNs containing POPC, DMPG, or DMPC lipids. The "PCFT" lane reactions did not contain any LPNs.

detected for reactions with LPNs containing the saturated lipids DMPG or DMPC as compared to those containing unsaturated POPC.

## DMPG and DMPC LPNs produce soluble PCFT

To further assess the impact of LPNs, their concentrations, and lipid compositions on the PCFT solubility, the experiment in Fig 3B was repeated with higher concentrations of LPNs, i.e., 80 μM LPNs, containing POPC, DMPG, and DMPC lipids (Fig 4A). 'PCFT' lanes
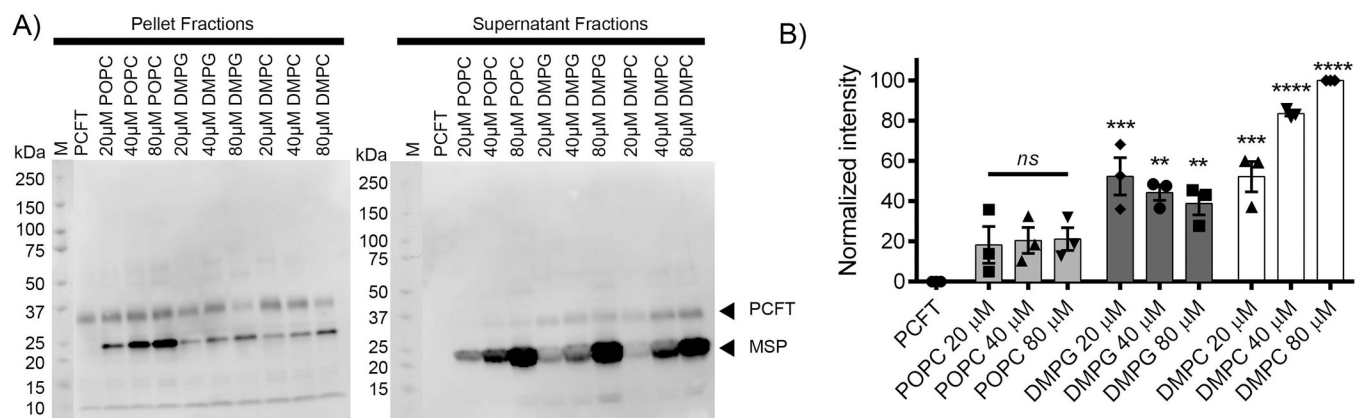


**Fig 4. Solubilization of PCFT in different lipid concentrations and compositions.** A) Cell-free expression of PCFT in the presence of 20 μM, 40 μM, or 80 μM LPNs containing POPC, DMPG, or DMPC lipid. PCFT lane did not contain any LPNs. The PCFT arrow indicates PCFT protein bands, and the MSP arrow indicates membrane scaffold protein (MSP) of LPNs. B) PCFT solubilization in 20 μM, 40 μM, or 80 μM LPNs containing POPC, DMPG, or DMPC lipid. The PCFT band intensity was quantified in western blots of supernatant fractions and normalized to the PCFT band derived from 80 μM DMPC LPNs. The data show the mean ± SEM from n = 3 independent experiments. The highest level of solubilized PCFT was found in LPNs containing DMPC lipid. LPNs containing POPC lipid yielded minimal levels of solubilized PCFT. Statistical significance was determined using was determined using one-way ANOVA with Tukey's multiple-comparisons test in Prism 6 Software (GraphPad Prism). Significance is indicated vs "PCFT" sample without LPNs as ** $p \leq 0.01$, *** $p \leq 0.001$, and $p \leq$ ****$0.0001$). Nonsignificant p value is shown as ns.

represent PCFT expressed in the absence of LPNs, and the lack of soluble PCFT again confirms that without LPNs, only insoluble PCFT was obtained in the cell-free expression. In contrast, depending on the specific lipid within LPNs, both insoluble and soluble PCFT were observed when LPNs were present during transcription and translation in the expression reaction. No or minimal PCFT was incorporated into POPC LPNs. For all three POPC LPN concentrations used, 20, 40, and 80 μM, when the band intensity was assessed using one-way ANOVA with Tukey's multiple-comparisons test, the PCFT band intensities were not significantly different from PCFT expressed in the absence of any solubilizing agent. At a concentration of 20 μM, DMPG LPNs yielded approximately three times the soluble PCFT intensity as compared to POPC LPNs. The soluble PCFT in DMPG reactions was significantly above the reactions without LPNs ($p \leq 0.001$, $p \leq 0.01$, $p \leq 0.01$ for 20, 40, and 80 μM, respectively). However, the concentration of the DMPG LPNs itself did not impact the soluble PCFT in a concentration-dependent manner.

Similar to 20 μM DMPG LPNs, the same concentration of 20 μM DMPC yielded a three-fold increase in soluble PCFT as compared to POPC LPNs. Contrary to DMPG LPNs, DMPC LPNs led to a concentration-dependent increase in soluble PCFT. The highest concentration of DMPC LPNs of 80 μM, produced the highest amount of soluble PCFT, approximately two-fold higher than all DMPC concentrations.

For downstream applications for which purified PCFT/nanodisc complexes are required, PCFT would be expressed as described here with the N-terminal His-tag in the presence of nanodiscs stabilized by MSP without His-tag. Metal affinity chromatography against the His-tag of PCFT while using untagged MSP nanodiscs and/or a gel filtration would provide scalable pathways to purified PCFT-LPNs complexes for downstream assays. Some biophysical measurements, for example single-molecule fluorescence resonance energy transfer (smFRET) measurements using Cys pairs labeled with appropriate donor and acceptor fluorophores within PCFT do not require purification [49–52].

Overall, incorporation of PCFT into LPNs containing DMPG and DMPC (the more ordered or condensed lipids compared to POPC [53]) was higher than compared to POPC LPNs with an overall increase in solubility from POPC < DMPG < DMPC. PCFT has been found in lipids rafts. Reduced levels in lipid rafts have been associated with folate malabsorption in chronic alcoholism [54]. Changes to the lipid raft composition in cancer have been implicated in regulating cell proliferation, apoptosis, and cell migration [55]. Lipid rafts are microdomains found in the plasma membrane that are enriched in sphingolipids and cholesterol. High levels of cholesterol in membranes lead to directional organization of the lipid bilayer due to the rigid sterol [56]. The packing of cholesterol in between lipid acyl chains consequently results in a closer packing or compaction of the lipid bilayer, a state of the bilayer also termed as "liquid-ordered". Therefore, the preference of PCFT to integrate into LPNs containing ordered lipids is comparable to its native localization within lipid raft microdomains.

## Conclusion

PCFT was identified as the main pathway for dietary folate uptake in the proximal small intestine in 2006 [5]. Detailed studies of human PCFT using PCFT constructs modified with amino acids engineered at specific positions, including the use of the substituted cysteine accessibly method (SCAM) [57] as well as recent cryo-EM structures of chicken PCFT have provided insights into the topology and conformational transitions during substrate translocation [15, 17, 33–40, 45, 58–61]. However, much remains unknown about PCFT's detailed molecular structure, substrate translocation mechanism, and lipid dependence. Structures of chicken PCFT were published in a substrate free state and in complex with the antifolate drug

pemetrexed [45]. PCFT adopts the outward-facing conformation in both structures. The PCFT cryo-EM structure obtained in the absence of substrate (PDB entry: 7BC6) in the outward-open state is largely similar to our published human PCFT 3D homology model based on the YajR experimental structure (PDB entry: 3WDO), with a root-mean-square deviation (RMSD) of 4.0Å [33, 35]. The substrate binding site as well as positions involved in functional aspects of PCFT are remarkably similar between our model and the experimental structure. In particular, the engagement of motif A (Asp109-Arg113-Asp170) is observed in both the cryo-EM structure and our 3WDO-based model, as would be expected in the outward-facing conformation. The cryo-EM structures were obtained using a nanobody that binds to the long extracellular loop between TM1 and TM2. The high affinity (KD of 8 nM) of the nanobody indicates its tight interactions with PCFT and at the same time provides the potential for structural disturbances based on the nanobody's interactions with extracellular loops and its insertion into the outward-facing substrate translocation pathway. These highly novel experimental structures further support our models but lack information pertaining to structural and functional changes occurring with disease causing mutations or conformational transitions caused by interaction with different substrates (folates vs antifolates). In particular, dynamic insights are lacking that could be obtained using smFRET experiments obtained with PCFT expressed as described in the present study. In addition, detailed structural information about the inward-open conformation, as well as occluded intermediate conformations in the transport cycle are still lacking.

The structure and activity of integral membrane proteins heavily depends on lipid environments [62–69] as demonstrated by the following select MFS transporter examples. For purine transporters, UapA and AzgA, it was shown that ergosterol, sphingolipids or phosphoinositides negatively affect biogenesis and stability of the transporters [70]. In the case of the secondary active transporter XylE, phosphatidylethanolamine has been demonstrated to disrupt conserved charge networks leading to conformational changes between different states and to favor an inward-facing state [71]. It was found that the transport activity of lysine transporter Lyp1 depends on the concentration of phosphatidylserine and ergosterol, while the transport rate of aspartate transporter relies on lipid composition [72, 73].

In this study, PCFT was produced in a soluble form using cell-free synthesis in the presence of membrane-mimicking LPNs. Soluble PCFT was obtained with a continuous one-step reaction and within one hour with an overall increase in solubility from POPC < DMPG < DMPC. In preliminary experiments, detergent micelles alone or mixed detergent-lipid micelles did not support soluble PCFT synthesis (S1 Fig). The described soluble PCFT expression directly into LPNs facilitates the expression of engineered constructs with site-specific modifications. In addition, the lipid composition can be systematically modified further. The expression level is amenable for diverse biophysical approaches to study PCFT's structure and function, such as applications using fluorescence (tryptophan fluorescence or smFRET), cryo-EM, isothermal titration calorimetry or circular dichroism.

## Supporting information

**S1 Fig.**
(TIF)

**S1 File.**
(DOCX)

**S1 Raw images.**
(PDF)

## Acknowledgments

## Author Contributions

**Conceptualization:** Michaela Jansen.

**Formal analysis:** Hoa Quynh Do.

**Funding acquisition:** Michaela Jansen.

**Investigation:** Carla M. Bassil, Elizabeth I. Andersen.

**Methodology:** Carla M. Bassil, Elizabeth I. Andersen.

**Project administration:** Michaela Jansen.

**Resources:** Michaela Jansen.

**Supervision:** Michaela Jansen.

**Visualization:** Hoa Quynh Do.

**Writing – original draft:** Hoa Quynh Do, Michaela Jansen.

**Writing – review & editing:** Hoa Quynh Do, Carla M. Bassil, Elizabeth I. Andersen, Michaela Jansen.

## References

1. Vinnicombe HG, Derrick JP. Dihydropteroate synthase: an old drug target revisited. Biochem Soc Trans. 1999; 27(2):53–8. Epub 1999/03/27. https://doi.org/10.1042/bst0270053 PMID: 10093706.

2. Elnakat H, Ratnam M. Distribution, functionality and gene regulation of folate receptor isoforms: implications in targeted therapy. Adv Drug Deliv Rev. 2004; 56(8):1067–84. Epub 2004/04/20. https://doi.org/10.1016/j.addr.2004.01.001 PMID: 15094207.

3. Matherly LH, Goldman DI. Membrane transport of folates. Vitam Horm. 2003; 66:403–56. Epub 2003/07/11. https://doi.org/10.1016/s0083-6729(03)01012-4 PMID: 12852262.

4. Matherly LH, Hou Z, Deng Y. Human reduced folate carrier: translation of basic biology to cancer etiology and therapy. Cancer Metastasis Rev. 2007; 26(1):111–28. Epub 2007/03/06. https://doi.org/10.1007/s10555-007-9046-2 PMID: 17334909.

5. Qiu AD, Jansen M, Sakaris A, Min SH, Chattopadhyay S, Tsai E, et al. Identification of an intestinal folate transporter and the molecular basis for hereditary folate malabsorption. Cell. 2006; 127(5):917–28. https://doi.org/10.1016/j.cell.2006.09.041 PubMed Central PMCID: PMC17129779. PMID: 17129779

6. Umapathy NS, Gnana-Prakasam JP, Martin PM, Mysona B, Dun Y, Smith SB, et al. Cloning and functional characterization of the proton-coupled electrogenic folate transporter and analysis of its expression in retinal cell types. Investigative Ophthalmology & Visual Science. 2007; 48(11):5299–305. https://doi.org/10.1167/iovs.07-0288 PubMed PMID: WOS:000250734800057. PMID: 17962486

7. Zhao R, Goldman ID. The molecular identity and characterization of a Proton-coupled Folate Transporter—PCFT; biological ramifications and impact on the activity of pemetrexed. Cancer Metastasis Rev. 2007; 26(1):129–39. Epub 2007/03/07. https://doi.org/10.1007/s10555-007-9047-1 PMID: 17340171.

8. Inoue K, Nakai Y, Ueda S, Kamigaso S, Ohta KY, Hatakeyama M, et al. Functional characterization of PCFT/HCP1 as the molecular entity of the carrier-mediated intestinal folate transport system in the rat model. Am J Physiol-Gastr L. 2008; 294(3):G660–G8. https://doi.org/10.1152/ajpgi.00309.2007 PubMed PMID: WOS:000253992200009. PMID: 18174275

9. Urquhart BL, Gregor JC, Chande N, Knauer MJ, Tirona RG, Kim RB. The human proton-coupled folate transporter (hPCFT): modulation of intestinal expression and function by drugs. Am J Physiol Gastrointest Liver Physiol. 2010; 298(2):G248–54. Epub 2009/09/19. https://doi.org/10.1152/ajpgi.00224.2009 PMID: 19762432.

10. Qiu A, Min SH, Jansen M, Malhotra U, Tsai E, Cabelof DC, et al. Rodent intestinal folate transporters (SLC46A1): secondary structure, functional properties, and response to dietary folate restriction. American Journal of Physiology-Cell Physiology. 2007; 293(5):C1669–C78. https://doi.org/10.1152/ajpcell.00202.2007 PubMed PMID: WOS:000250709500026. PMID: 17898134

11. Zhao R, Min SH, Wang Y, Campanella E, Low PS, Goldman ID. A role for the proton-coupled folate transporter (PCFT-SLC46A1) in folate receptor-mediated endocytosis. J Biol Chem. 2009; 284 (7):4267–74. https://doi.org/10.1074/jbc.M807665200 PMID: 19074442; PubMed Central PMCID: PMC2640977.

12. Wollack JB, Makori B, Ahlawat S, Koneru R, Picinich SC, Smith A, et al. Characterization of folate uptake by choroid plexus epithelial cells in a rat primary culture model. J Neurochem. 2008; 104 (6):1494–503. Epub 2007/12/19. https://doi.org/10.1111/j.1471-4159.2007.05095.x PMID: 18086128.

13. Zhao R, Goldman ID. The proton-coupled folate transporter: physiological and pharmacological roles. Curr Opin Pharmacol. 2013; 13(6):875–80. Epub 2014/01/03. https://doi.org/10.1016/j.coph.2013.09.011 PMID: 24383099; PubMed Central PMCID: PMC4100332.

14. Geller J, Kronn D, Jayabose S, Sandoval C. Hereditary folate malabsorption: family report and review of the literature. Medicine (Baltimore). 2002; 81(1):51–68. Epub 2002/01/25. https://doi.org/10.1097/00005792-200201000-00004 PMID: 11807405.

15. Mahadeo K, Diop-Bove N, Shin D, Unal ES, Teo J, Zhao R, et al. Properties of the Arg376 residue of the proton-coupled folate transporter (PCFT-SLC46A1) and a glutamine mutant causing hereditary folate malabsorption. Am J Physiol Cell Physiol. 2010; 299(5):C1153–61. Epub 2010/08/06. doi: ajp-cell.00113.2010 [pii] 10.1152/ajpcell.00113.2010. https://doi.org/10.1152/ajpcell.00113.2010 PMID: 20686069; PubMed Central PMCID: PMC2980313.

16. Meyer E, Kurian MA, Pasha S, Trembath RC, Cole T, Maher ER. A novel PCFT gene mutation (p. Cys66LeufsX99) causing hereditary folate malabsorption. Mol Genet Metab. 2010; 99(3):325–8. https://doi.org/10.1016/j.ymgme.2009.11.004 PMID: 20005757; PubMed Central PMCID: PMC2852677.

17. Shin DS, Zhao R, Fiser A, Goldman DI. Functional roles of the A335 and G338 residues of the proton-coupled folate transporter (PCFT-SLC46A1) mutated in hereditary folate malabsorption. Am J Physiol Cell Physiol. 2012; 303(8):C834–42. https://doi.org/10.1152/ajpcell.00171.2012 PMID: 22843796; PubMed Central PMCID: PMC3469714.

18. Shin DS, Mahadeo K, Min SH, Diop-Bove N, Clayton P, Zhao R, et al. Identification of novel mutations in the proton-coupled folate transporter (PCFT-SLC46A1) associated with hereditary folate malabsorption. Mol Genet Metab. 2011; 103(1):33–7. Epub 2011/02/22. doi: S1096-7192(11)00033-3 [pii] 10.1016/j.ymgme.2011.01.008. https://doi.org/10.1016/j.ymgme.2011.01.008 PMID: 21333572; PubMed Central PMCID: PMC3081934.

19. Borzutzky A, Crompton B, Bergmann AK, Giliani S, Baxi S, Martin M, et al. Reversible severe combined immunodeficiency phenotype secondary to a mutation of the proton-coupled folate transporter. Clin Immunol. 2009; 133(3):287–94. Epub 2009/09/11. https://doi.org/10.1016/j.clim.2009.08.006 PMID: 19740703; PubMed Central PMCID: PMC2783538.

20. Kronn D, Goldman ID. Hereditary Folate Malabsorption. In: Adam MP, Ardinger HH, Pagon RA, Wallace SE, Bean LJH, Stephens K, et al., editors. GeneReviews((R)). Seattle (WA)1993.

21. Manea E, Gissen P, Pope S, Heales SJ, Batzios S. Role of Intramuscular Levofolinate Administration in the Treatment of Hereditary Folate Malabsorption: Report of Three Cases. JIMD Rep. 2018; 39:7–12. Epub 2017/07/08. https://doi.org/10.1007/8904_2017_39 PMID: 28685492; PubMed Central PMCID: PMC5953899.

22. Snowdon DA, Tully CL, Smith CD, Riley KP, Markesbery WR. Serum folate and the severity of atrophy of the neocortex in Alzheimer disease: findings from the Nun Study. Am J Clin Nutr. 2000; 71(4):993–8. PubMed PMID: WOS:000086064400021. https://doi.org/10.1093/ajcn/71.4.993 PMID: 10731508

23. Serot JM, Christmann D, Dubost T, Bene MC, Faure GC. CSF-folate levels are decreased in late-onset AD patients. J Neural Transm. 2001; 108(1):93–9. https://doi.org/10.1007/s007020170100 PubMed PMID: WOS:000166717200010. PMID: 11261750

24. Smach MA, Jacob N, Golmard JL, Charfeddine B, Lammouchi T, Ben Othman L, et al. Folate and Homocysteine in the Cerebrospinal Fluid of Patients with Alzheimer's Disease or Dementia: A Case Control Study. Eur Neurol. 2011; 65(5):270–8. https://doi.org/10.1159/000326301 PubMed PMID: WOS:000290580500005. PMID: 21474939

25. Liu H, Tian T, Qin SC, Li W, Zhang XM, Wang X, et al. Folic acid deficiency enhances abeta accumulation in APP/PS1 mice brain and decreases amyloid-associated miRNAs expression. J Nutr Biochem. 2015; 26(12):1502–8. https://doi.org/10.1016/j.jnutbio.2015.07.020 PubMed PMID: WOS:000366785600011. PMID: 26345540

**26.** Chan A, Shea TB. Folate deprivation increases presenilin expression, gamma-secretase activity, and Abeta levels in murine brain: potentiation by ApoE deficiency and alleviation by dietary S-adenosyl methionine. J Neurochem. 2007; 102(3):753–60. Epub 2007/05/17. https://doi.org/10.1111/j.1471-4159.2007.04589.x PMID: 17504266.

**27.** Ramaekers VT, Blau N. Cerebral folate deficiency. Dev Med Child Neurol. 2004; 46(12):843–51. Epub 2004/12/08. https://doi.org/10.1017/s0012162204001471 PMID: 15581159.

**28.** Pineda M, Ormazabal A, Lopez-Gallardo E, Nascimento A, Solano A, Herrero MD, et al. Cerebral folate deficiency and leukoencephalopathy caused by a mitochondrial DNA deletion. Ann Neurol. 2006; 59 (2):394–8. Epub 2005/12/21. https://doi.org/10.1002/ana.20746 PMID: 16365882.

**29.** Torres A, Newton SA, Crompton B, Borzutzky A, Neufeld EJ, Notarangelo L, et al. CSF 5-Methyltetrahy-drofolate Serial Monitoring to Guide Treatment of Congenital Folate Malabsorption Due to Proton-Cou-pled Folate Transporter (PCFT) Deficiency. Ann Neurol. 2015; 78:S199–S200. PubMed PMID: WOS:000362668600474. https://doi.org/10.1007/8904_2015_445 PMID: 26006721

**30.** Min SH, Oh SY, Karp GI, Poncz M, Zhao R, Goldman ID. The clinical course and genetic defect in the PCFT gene in a 27-year-old woman with hereditary folate malabsorption. J Pediatr. 2008; 153(3):435–7. Epub 2008/08/23. doi: S0022-3476(08)00272-2 [pii] 10.1016/j.jpeds.2008.04.009. https://doi.org/10.1016/j.jpeds.2008.04.009 PMID: 18718264.

**31.** Sierra EE, Goldman ID. Characterization of folate transport mediated by a low pH route in mouse L1210 leukemia cells with defective reduced folate carrier function. Biochem Pharmacol. 1998; 55(9):1505–12. Epub 1999/03/17. https://doi.org/10.1016/s0006-2952(97)00673-4 PMID: 10076544.

**32.** Kugel Desmoulin S, Wang L, Hales E, Polin L, White K, Kushner J, et al. Therapeutic targeting of a novel 6-substituted pyrrolo [2,3-d]pyrimidine thienoyl antifolate to human solid tumors based on selec-tive uptake by the proton-coupled folate transporter. Mol Pharmacol. 2011; 80(6):1096–107. Epub 2011/09/24. https://doi.org/10.1124/mol.111.073833 PMID: 21940787; PubMed Central PMCID: PMC3228537.

**33.** Duddempudi PK, Goyal R, Date SS, Jansen M. Delineating the extracellular water-accessible surface of the proton-coupled folate transporter. PLoS One. 2013; 8(10):e78301. Epub 2013/11/10. https://doi.org/10.1371/journal.pone.0078301 PMID: 24205192; PubMed Central PMCID: PMC3799626.

**34.** Duddempudi PK, Nakashe P, Blanton MP, Jansen M. The monomeric state of the proton-coupled folate transporter represents the functional unit in the plasma membrane. FEBS J. 2013; 280(12):2900–15. https://doi.org/10.1111/febs.12293 PMID: 23601781.

**35.** Date SS, Chen CY, Chen Y, Jansen M. Experimentally optimized threading structures of the proton-coupled folate transporter. FEBS Open Bio. 2016; 6(3):216–30. Epub 2016/04/06. https://doi.org/10.1002/2211-5463.12041 PMID: 27047750; PubMed Central PMCID: PMC4794783.

**36.** Aluri S, Zhao R, Fiser A, Goldman ID. Substituted-cysteine accessibility and cross-linking identify an exofacial cleft in the 7th and 8th helices of the proton-coupled folate transporter (SLC46A1). Am J Phy-siol Cell Physiol. 2018; 314(3):C289–C96. Epub 2017/11/24. https://doi.org/10.1152/ajpcell.00215.2017 PMID: 29167151; PubMed Central PMCID: PMC6415652.

**37.** Aluri S, Zhao R, Fiser A, Goldman ID. Residues in the eighth transmembrane domain of the proton-cou-pled folate transporter (SLC46A1) play an important role in defining the aqueous translocation pathway and in folate substrate binding. Biochim Biophys Acta Biomembr. 2017; 1859(11):2193–202. Epub 2017/08/15. https://doi.org/10.1016/j.bbamem.2017.08.006 PMID: 28802835; PubMed Central PMCID: PMC5624325.

**38.** Aluri S, Zhao R, Lin K, Shin DS, Fiser A, Goldman ID. Substitutions that lock and unlock the proton-cou-pled folate transporter (PCFT-SLC46A1) in an inward-open conformation. J Biol Chem. 2019. Epub 2019/03/13. https://doi.org/10.1074/jbc.RA118.005533 PMID: 30858177.

**39.** Zhao R, Najmi M, Fiser A, Goldman ID. Identification of an Extracellular Gate for the Proton-coupled Folate Transporter (PCFT-SLC46A1) by Cysteine Cross-linking. J Biol Chem. 2016; 291(15):8162–72. Epub 2016/02/18. https://doi.org/10.1074/jbc.M115.693929 PMID: 26884338; PubMed Central PMCID: PMC4825018.

**40.** Shin DS, Zhao R, Fiser A, Goldman ID. The Role of the Fourth Transmembrane Domain in Proton-Cou-pled Folate Transporter (PCFT) Function as Assessed by the Substituted Cysteine Accessibility Method. Am J Physiol Cell Physiol. 2013. https://doi.org/10.1152/ajpcell.00353.2012 PMID: 23552283.

**41.** Desmoulin SK, Hou ZJ, Gangjee A, Matherly LH. The human proton-coupled folate transporter Biology and therapeutic applications to cancer. Cancer Biol Ther. 2012; 13(14):1355–73. https://doi.org/10.4161/cbt.22020 PubMed PMID: WOS:000312212200002. PMID: 22954694

**42.** Cherian C, Kugel Desmoulin S, Wang L, Polin L, White K, Kushner J, et al. Therapeutic targeting malig-nant mesothelioma with a novel 6-substituted pyrrolo[2,3-d]pyrimidine thienoyl antifolate via its selective uptake by the proton-coupled folate transporter. Cancer Chemother Pharmacol. 2013; 71(4):999–1011.

Epub 2013/02/16. https://doi.org/10.1007/s00280-013-2094-0 PMID: 23412628; PubMed Central PMCID: PMC3769948.

43. Wilson MR, Hou Z, Yang S, Polin L, Kushner J, White K, et al. Targeting Nonsquamous Nonsmall Cell Lung Cancer via the Proton-Coupled Folate Transporter with 6-Substituted Pyrrolo[2,3-d]Pyrimidine Thienoyl Antifolates. Mol Pharmacol. 2016; 89(4):425–34. Epub 2016/02/04. https://doi.org/10.1124/mol.115.102798 PMID: 26837243; PubMed Central PMCID: PMC4809305.

44. Zhao R, Qiu A, Tsai E, Jansen M, Akabas MH, Goldman ID. The proton-coupled folate transporter: impact on pemetrexed transport and on antifolates activities compared with the reduced folate carrier. Mol Pharmacol. 2008; 74(3):854–62. Epub 2008/06/06. doi: mol.108.045443 [pii] 10.1124/mol.108.045443. https://doi.org/10.1124/mol.108.045443 PMID: 18524888.

45. Parker JL, Deme JC, Kuteyi G, Wu Z, Huo J, Goldman ID, et al. Structural basis of antifolate recognition and transport by PCFT. Nature. 2021. Epub 2021/05/28. https://doi.org/10.1038/s41586-021-03579-z PMID: 34040256.

46. Newby ZE, O'Connell JD 3rd, Gruswitz F, Hays FA, Harries WE, Harwood IM, et al. A general protocol for the crystallization of membrane proteins for X-ray structural investigation. Nat Protoc. 2009; 4 (5):619–37. Epub 2009/04/11. https://doi.org/10.1038/nprot.2009.27 PMID: 19360018; PubMed Central PMCID: PMC4075773.

47. Hou ZJ, Desmoulin SK, Etnyre E, Olive M, Hsiung B, Cherian C, et al. Identification and Functional Impact of Homo-oligomers of the Human Proton-coupled Folate Transporter. Journal of Biological Chemistry. 2012; 287(7):4982–95. https://doi.org/10.1074/jbc.M111.306860 PubMed PMID: WOS:000300608500058. PMID: 22179615

48. Unal ES, Zhao RB, Qiu AD, Goldman ID. N-linked glycosylation and its impact on the electrophoretic mobility and function of the human proton-coupled folate transporter (HsPCFT). Biochimica Et Biophysica Acta-Biomembranes. 2008; 1778(6):1407–14. https://doi.org/10.1016/j.bbamem.2008.03.009 PubMed PMID: WOS:000256655800005. PMID: 18405659

49. Sirrieh RE, MacLean DM, Jayaraman V. A conserved structural mechanism of NMDA receptor inhibition: A comparison of ifenprodil and zinc. J Gen Physiol. 2015; 146(2):173–81. Epub 2015/07/15. https://doi.org/10.1085/jgp.201511422 PMID: 26170175; PubMed Central PMCID: PMC4516779.

50. Dolino DM, Chatterjee S, MacLean DM, Flatebo C, Bishop LDC, Shaikh SA, et al. The structure-energy landscape of NMDA receptor gating. Nat Chem Biol. 2017; 13(12):1232–8. Epub 2017/10/11. https://doi.org/10.1038/nchembio.2487 PMID: 28991238; PubMed Central PMCID: PMC5698143.

51. Shaikh SA, Dolino DM, Lee G, Chatterjee S, MacLean DM, Flatebo C, et al. Stargazin Modulation of AMPA Receptors. Cell reports. 2016; 17(2):328–35. Epub 2016/10/06. https://doi.org/10.1016/j.celrep.2016.09.014 PMID: 27705782; PubMed Central PMCID: PMC5088782.

52. MacLean DM, Durham RJ, Jayaraman V. Mapping the Conformational Landscape of Glutamate Receptors Using Single Molecule FRET. Trends in neurosciences. 2019; 42(2):128–39. Epub 2018/11/06. https://doi.org/10.1016/j.tins.2018.10.003 PMID: 30385052; PubMed Central PMCID: PMC6359962.

53. Small DM. Lateral chain packing in lipids and membranes. Journal of lipid research. 1984; 25 (13):1490–500. Epub 1984/12/15. PMID: 6530598.

54. Wani NA, Kaur J. Reduced levels of folate transporters (PCFT and RFC) in membrane lipid rafts result in colonic folate malabsorption in chronic alcoholism. Journal of cellular physiology. 2011; 226(3):579–87. https://doi.org/10.1002/jcp.22525 PMID: 21069807.

55. Gueguinou M, Gambade A, Felix R, Chantome A, Fourbon Y, Bougnoux P, et al. Lipid rafts, KCa/ClCa/Ca2+ channel complexes and EGFR signaling: Novel targets to reduce tumor development by lipids? Biochim Biophys Acta. 2015; 1848(10 Pt B):2603–20. https://doi.org/10.1016/j.bbamem.2014.10.036 PMID: 25450343.

56. Munro S. Lipid rafts: elusive or illusive? Cell. 2003; 115(4):377–88. Epub 2003/11/19. https://doi.org/10.1016/s0092-8674(03)00882-1 PMID: 14622593.

57. Akabas MH, Stauffer DA, Xu M, Karlin A. Acetylcholine receptor channel structure probed in cysteine-substitution mutants. Science. 1992; 258(5080):307–10. https://doi.org/10.1126/science.1384130 PMID: 1384130

58. Date SS, Fiori MC, Altenberg GA, Jansen M. Expression in Sf9 insect cells, purification and functional reconstitution of the human proton-coupled folate transporter (PCFT, SLC46A1). PLoS One. 2017; 12 (5):e0177572. Epub 2017/05/12. https://doi.org/10.1371/journal.pone.0177572 PMID: 28493963; PubMed Central PMCID: PMC5426777.

59. Aluri S, Zhao R, Lubout C, Goorden SMI, Fiser A, Goldman ID. Hereditary folate malabsorption due to a mutation in the external gate of the proton-coupled folate transporter SLC46A1. Blood Adv. 2018; 2 (1):61–8. Epub 2018/01/19. https://doi.org/10.1182/bloodadvances.2017012690 PMID: 29344585; PubMed Central PMCID: PMC5761628 interests.

60.   Shin DS, Zhao R, Yap EH, Fiser A, Goldman ID. A P425R mutation of the proton-coupled folate trans-
      porter causing hereditary folate malabsorption produces a highly selective alteration in folate binding.
      Am J Physiol Cell Physiol. 2012. Epub 2012/02/22. doi: ajpcell.00435.2011 [pii] 10.1152/ajp-
      cell.00435.2011. https://doi.org/10.1152/ajpcell.00435.2011 PMID: 22345511.

61.   Shin DS, Min SH, Russell L, Zhao R, Fiser A, Goldman ID. Functional roles of aspartate residues of the
      proton-coupled folate transporter (PCFT-SLC46A1); a D156Y mutation causing hereditary folate mal-
      absorption. Blood. 2010; 116(24):5162–9. Epub 2010/09/02. doi: blood-2010-06-291237 [pii] 10.1182/
      blood-2010-06-291237. https://doi.org/10.1182/blood-2010-06-291237 PMID: 20805364; PubMed
      Central PMCID: PMC3012536.

62.   Hu F, Luo W, Cady SD, Hong M. Conformational plasticity of the influenza A M2 transmembrane helix
      in lipid bilayers under varying pH, drug binding, and membrane thickness. Biochim Biophys Acta. 2011;
      1808(1):415–23. Epub 2010/10/05. https://doi.org/10.1016/j.bbamem.2010.09.014 PMID: 20883664;
      PubMed Central PMCID: PMC2997931.

63.   Liu SA, Focke PJ, Matulef K, Bian XL, Moenne-Loccoz P, Valiyaveetil FI, et al. Ion-binding properties of
      a K+ channel selectivity filter in different conformations. Proceedings of the National Academy of Sci-
      ences of the United States of America. 2015; 112(49):15096–100. https://doi.org/10.1073/pnas.
      1510526112 PubMed PMID: WOS:000365989800040. PMID: 26598654

64.   Singh DK, Shentu TP, Enkvetchakul D, Levitan I. Cholesterol regulates prokaryotic Kir channel by direct
      binding to channel protein. Biochim Biophys Acta. 2011; 1808(10):2527–33. Epub 2011/07/30. https://
      doi.org/10.1016/j.bbamem.2011.07.006 PMID: 21798234; PubMed Central PMCID: PMC3156940.

65.   Hansen SB, Tao X, MacKinnon R. Structural basis of PIP2 activation of the classical inward rectifier K+
      channel Kir2.2. Nature. 2011; 477(7365):495–8. Epub 2011/08/30. https://doi.org/10.1038/nature10370
      PMID: 21874019; PubMed Central PMCID: PMC3324908.

66.   Cheng WWL, D'Avanzo N, Doyle DA, Nichols CG. Dual-mode phospholipid regulation of human inward
      rectifying potassium channels. Biophys J. 2011; 100(3):620–8. Epub 2011/02/02. https://doi.org/10.
      1016/j.bpj.2010.12.3724 PMID: 21281576; PubMed Central PMCID: PMC3030149.

67.   Furst O, Mondou B, D'Avanzo N. Phosphoinositide regulation of inward rectifier potassium (Kir) chan-
      nels. Front Physiol. 2014; 4:404. Epub 2014/01/11. https://doi.org/10.3389/fphys.2013.00404 PMID:
      24409153; PubMed Central PMCID: PMC3884141.

68.   Lavington S, Watts A. Lipid nanoparticle technologies for the study of G protein-coupled receptors in
      lipid environments. Biophys Rev. 2020. Epub 2020/11/21. https://doi.org/10.1007/s12551-020-00775-5
      PMID: 33215301; PubMed Central PMCID: PMC7755959.

69.   Dijkman PM, Munoz-Garcia JC, Lavington SR, Kumagai PS, Dos Reis RI, Yin D, et al. Conformational
      dynamics of a G protein-coupled receptor helix 8 in lipid membranes. Sci Adv. 2020; 6(33):eaav8207.
      Epub 2020/08/28. https://doi.org/10.1126/sciadv.aav8207 PMID: 32851152; PubMed Central PMCID:
      PMC7428336.

70.   Dionysopoulou M, Diallinas G. Impact of Membrane Lipids on UapA and AzgA Transporter Subcellular
      Localization and Activity in Aspergillus nidulans. J Fungi (Basel). 2021; 7(7). Epub 2021/07/03. https://
      doi.org/10.3390/jof7070514 PMID: 34203131; PubMed Central PMCID: PMC8304608.

71.   Martens C, Shekhar M, Borysik AJ, Lau AM, Reading E, Tajkhorshid E, et al. Direct protein-lipid interac-
      tions shape the conformational landscape of secondary transporters. Nat Commun. 2018; 9(1):4151.
      Epub 2018/10/10. https://doi.org/10.1038/s41467-018-06704-1 PMID: 30297844; PubMed Central
      PMCID: PMC6175955.

72.   van 't Klooster JS, Cheng TY, Sikkema HR, Jeucken A, Moody DB, Poolman B. Membrane Lipid
      Requirements of the Lysine Transporter Lyp1 from Saccharomyces cerevisiae. J Mol Biol. 2020; 432
      (14):4023–31. Epub 2020/05/16. https://doi.org/10.1016/j.jmb.2020.04.029 PMID: 32413406; PubMed
      Central PMCID: PMC8005870.

73.   McIlwain BC, Vandenberg RJ, Ryan RM. Transport rates of a glutamate transporter homologue are
      influenced by the lipid bilayer. J Biol Chem. 2015; 290(15):9780–8. Epub 2015/02/26. https://doi.org/10.
      1074/jbc.M114.630590 PMID: 25713135; PubMed Central PMCID: PMC4392276.